Supplementary Information (SI) for ChemComm.
This journal is © The Royal Society of Chemistry 2026

Supplementary Information

Chiral Supramolecular Alloys: Programmable 2D–3D Control via Co-assembly of Isomorphous β-Peptide Foldamers

Yi Sak Park,[a,†] So-Mang Lee,[a,†] Sungmo Koo,[a] Jintaek Gong,[a,c] Jungwoo Hong,[a,b] Sung Hyun Yoo,*[a,d] and Hee-Seung Lee*[a,b]

[a]Department of Chemistry, Korea Advanced Institute of Science and Technology (KAIST), Daejeon 34141, Republic of Korea

[b]InnoCORE AI Co-Research & Education for Innovative Drug (AI-CRED) Institute, KAIST, Daejeon 34141, Republic of Korea

[c]Department of Chemistry Education, Sunchon National University, Suncheon 57922, Republic of Korea

[d]Department of Chemistry, Chonnam National University, Gwangju 61186, Republic of Korea

[†]These authors contributed equally to this work.

*sunghyun.yoo@jnu.ac.kr and hee-seung_lee@kaist.ac.kr

Table of contents

Materials and methods S3

Materials S3

Synthesis of β-peptides S3

Procedure for self-assembly S4

Characterization methods S4

Nuclear magnetic resonance spectroscopy (NMR) S4

High-resolution mass spectrometry (HRMS) S4

Scanning electron microscopy (SEM) S4

Selected area electron diffraction (SAED) S4

Atomic force microscopy (AFM) S4

Circular dichroism (CD) S4

High-performance liquid chromatography (HPLC) S5

Single crystal X-ray diffraction of $\mathbf{P_1}$ S5

Powder X-ray diffraction (PXRD) experimental condition of $\mathbf{F_1}$ S5

PXRD data analysis of $\mathbf{F_1}$ S5

Supplementary figures S7

Supplementary tables S13

Supplementary references S17

Materials and methods

Materials

All materials for the synthesis of peptides and self-assembly studies were purchased from Sigma-Aldrich, Tokyo Chemical Industry (TCI), Acros, and Junsei. Before use, *N,N*-dimethylformamide (DMF) was vacuum distilled and stored over 4 Å molecular sieve under N_2 atmosphere. High-purity water was obtained using Milli-Q apparatus (Millipore). All reactions were conducted under N_2 atmosphere and monitored by thin layer chromatography (TLC) on Merck precoated silica gel 60 F254 glass plates. TLC monitoring was performed by exposure to UV light at 254 nm, followed by a standard staining process using ninhydrin, phosphomolybdic acid or *p*-anisaldehyde solutions. Purification of reaction mixtures was carried out by flash column chromatography using silica gel (Merck 60, 230–400 mesh). NMR solvents (chloroform-*d* and pyridine-d_5) were purchased from Sigma-Aldrich and Cambridge Isotope Laboratories.

Synthesis of β-peptides

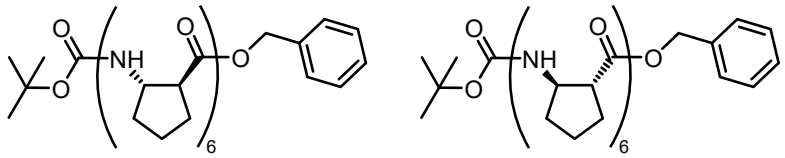

P_0 ***ent*-P_0**

P_0 and ***ent*-P_0**: These molecules were prepared following the reported procedures.[1-3]

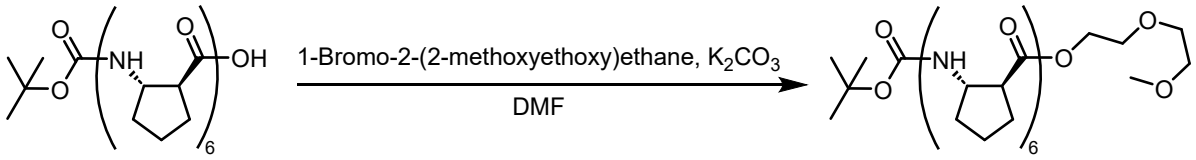

Boc-(S,S)-ACPC$_6$-OH **P_1**

P_1: To a stirred solution of Boc–(*S*,*S*)-ACPC$_6$–OH (0.12 g, 0.15 mmol)[4] in DMF (5 mL), K_2CO_3 (0.14 g, 0.075 mmol) and 1-bromo-2-(2-methoxyethoxy)ethane (0.060 mL, 0.45 mmol) dissolved in DMF (2 mL) were sequentially added under N_2. The reaction mixture was stirred at room temperature for 2 days. A saturated aqueous NH_4Cl solution was added to the reaction mixture, and the mixture was extracted with ethyl acetate. The organic layer was dried over $MgSO_4$ and the solvent was evaporated under reduced pressure. The crude product was purified by flash column chromatography using ethyl acetate as the eluent to afford the desired product (0.12 g, 93%).

^{1}H NMR (900 MHz, pyridine-d_5) δ 9.44 (d, *J* = 7.9 Hz, 1H), 9.07 (d, *J* = 8.9 Hz, 1H), 8.97 (d, *J* = 7.3 Hz, 1H), 8.85 (d, *J* = 8.3 Hz, 1H), 8.47 (d, *J* = 9.2 Hz, 1H), 8.40 (d, *J* = 8.1 Hz, 1H), 5.09 (ddd, *J* = 12.8, 7.4, 5.4 Hz, 1H), 4.94–4.87 (m, 2H), 4.81–4.73 (m, 2H), 4.54–4.47 (m, 2H), 4.35 (ddd, *J* = 11.7, 5.8, 4.1 Hz, 1H), 3.78–3.72 (m, 2H), 3.69–3.66 (m, 2H), 3.56 (dt, *J* = 9.2, 5.7 Hz, 1H), 3.54–3.51 (m, 2H), 3.28 (s, 3H), 3.23 (dt, *J* = 9.2, 6.2 Hz, 1H), 2.96–2.91 (m, 2H), 2.77 (q, *J* = 8.1 Hz, 1H), 2.66 (dt, *J* = 9.2, 7.1 Hz, 1H), 2.54 (dq, *J* = 13.6, 6.9 Hz, 1H), 2.46 (dq, *J* = 14.3, 7.5 Hz, 1H), 2.38 (dq, *J* = 14.3, 7.4 Hz, 1H), 2.31–2.13 (m, 5H), 2.12–1.85 (m, 15H), 1.85–1.65 (m, 12H), 1.57 (dq, *J* = 13.0, 6.8 Hz, 1H), 1.54 (s, 9H).
^{13}C NMR (126 MHz, chloroform-*d*) δ 175.93, 174.82, 174.66, 174.63, 174.61, 174.33, 156.34, 79.83, 72.04, 70.58, 69.26, 63.59, 59.14, 57.38, 55.45, 55.41, 55.40, 55.35, 54.53, 54.40, 53.25, 52.53, 52.50, 52.19, 50.26, 33.62, 33.60, 33.58, 33.57, 33.46, 32.56, 29.48, 29.42, 28.62, 28.53, 28.50, 28.42, 28.23, 25.22, 25.11, 24.91, 24.67, 23.80, 23.47.
HRMS (ESI+) calcd. for $C_{46}H_{74}N_6O_{11}Na$ $[M+Na]^+$ 909.5308, found 909.5314.

Procedure for self-assembly

Self-assembly of P_0 for F_0: A $\mathbf{P_0}$ solution in THF (50 µL, 4 mg mL^{-1}) was added to an aqueous solution of Pluronic P123 (1 mL, 8 g L^{-1}) and stirred vigorously at room temperature for 3 minutes. The solution was allowed to stand at room temperature for 3 hours. Afterward, the resulting mixture was centrifuged at 8000 rpm for 3 minutes. The supernatant was decanted, and the precipitate was collected. The precipitate was washed with distilled water (1 mL) three times.

Self-assembly of P_1 for F_1: A $\mathbf{P_1}$ solution in THF (50 µL, 10 mg mL^{-1}) was added to an aqueous solution of Pluronic P123 (0.5 mL, 10 g L^{-1}) and stirred vigorously at room temperature for 1 minute. The solution was allowed to stand at room temperature for 3 hours. Afterward, the resulting mixture was centrifuged at 3600 rpm for 3 minutes. The supernatant was decanted, and the precipitate was collected. The precipitate was washed with distilled water (1 mL) three times.

Co-assembly of P_0 and P_1: The mixed peptide solution was prepared by adding $\mathbf{P_1}$ in a ratio of [$\mathbf{P_1}$]:[$\mathbf{P_0}$] from 0:1 to 1:1, with the $\mathbf{P_0}$ solution fixed in THF (50 µL, 4 mg mL^{-1}). THF was added to adjust the total peptide solution to a final volume of 70 µL. The peptide solution in THF (70 µL) was added to an aqueous solution of Pluronic P123 (1 mL, 8 g L^{-1}) and stirred vigorously at room temperature for 1 minute. The solution was allowed to stand at room temperature for 3 hours. Afterward, the mixture was centrifuged at 3600 rpm for 3 minutes, and the precipitate was collected. To remove THF and residual P123, the precipitate was washed three times with distilled water. For the co-assembly of ***ent*-$\mathbf{P_0}$** and $\mathbf{P_1}$, the same procedure was followed using ***ent*-$\mathbf{P_0}$** instead of $\mathbf{P_0}$.

Co-assembly in CTAB solution: The procedure is identical to the co-assembly of $\mathbf{P_0}$ and $\mathbf{P_1}$, except for using an aqueous solution of CTAB (1 mL, 5 g L^{-1}) instead of Pluronic P123 (1 mL, 8 g L^{-1}).

Characterization methods

Nuclear magnetic resonance spectroscopy (NMR)

^1H and ^{13}C nuclear magnetic resonance (NMR) spectra were obtained with Bruker AVANCE II (900 MHz for ^1H NMR), Bruker AV500 (126 MHz for ^{13}C NMR) and measured in chloroform-*d* or pyridine-d_5. Chemical shifts were recorded as parts per million (ppm) relative to the residual solvent signal of chloroform-*d* (δ_C = 77.16 ppm) or pyridine-d_5 (δ_H = 8.74 ppm) [multiplicity (s = singlet, d = doublet, t = triplet, q = quartet, m = multiplet)] and coupling constants were reported in Hertz (Hz).

High-resolution mass spectrometry (HRMS)

HRMS spectra were recorded on micrOTOF-Q (Bruker, USA) spectrometer from KARA (KAIST Analysis Center for Research Advancement) by using the ESI-positive method.

Scanning electron microscopy (SEM)

SEM images were obtained by using Inspect F50 (Czech Republic), FEI at an accelerating voltage of 10 kV, after Pt coating using sputter coater 108 auto (Cressington Scientific Instruments).

Selected area electron diffraction (SAED)

SAED pattern was obtained by using Cryo Field Emission TEM (200kV, Thermo Fisher Glacios, USA) at liquid nitrogen temperature.

Atomic force microscopy (AFM)

AFM image was obtained by using Scanning Probe Microscope (XE-100, Park System, Korea) in non-contact mode.

Circular dichroism (CD)

CD spectra were recorded on a Jasco J-815 spectrophotometer (Jasco. Inc., Japan) in the range of 190–260 nm. CD samples were prepared in methanol (1 mM) in 0.1 mm quartz cell.

High-performance liquid chromatography (HPLC)

HPLC data were obtained using an analytical HPLC (Dionex, P680 HPLC pump, ASI-100 auto sample injector, UVD 170U, UV detector wavelength at 220 nm) equipped with a ProntoSIL column (120-5 C18 SH, Column 250 x 4.6 mm). A gradient of 5–95% acetonitrile in MQ water over 60 minutes at a column temperature of 40 °C was applied.

Single crystal X-ray diffraction of P_1

Single crystals of **P_1** were grown by slow diffusion (diethyl ether/chloroform) and diffraction data was collected on a Bruker D8 VENTURE instrument with graphite-monochromated MoKα radiation (λ = 0.71073 Å) under a stream of N_2 (g) at 200 K. Data were collected using *φ* and *ω* scans to a maximum θ of 28.385°, corresponding to a resolution of *ca* 0.75 Å, with 99.4% completeness to θ_{max} (99.3% complete to θ_{full} = 25.242°). The diffraction data were essentially complete; however, the final refinement required numerous restraints, consistent with disorder and limited data quality in parts of the structure. Cell parameters were determined and subsequently refined by SMART.[5] An empirical absorption correction was applied using the SADABS program.[6] The structure was solved using SHELXD[7] and refined by full-matrix least-squares on F^2 using SHELXL[8]-2025/1 within Olex2.[9] Non-hydrogen atoms were refined anisotropically where possible, with additional restraints applied to disordered regions. Hydrogen atoms were placed in calculated positions and refined using a riding model. The crystallographic information used for single crystal X-ray analysis of **P_1** is in Table S1.

Powder X-ray diffraction (PXRD) experimental condition of F_1

Samples for powder X-ray diffraction were prepared by repeating the self-assembly experiment procedures performed in our laboratory. The synchrotron diffraction data of **F_1** was collected at the 9B High-resolution Powder Diffraction beamline of Pohang Accelerator Laboratory (PAL, Pohang, Republic of Korea) using monochromatic radiation (λ=1.48630 Å). A flat polycarbonate holder was used as the sample holder. The pattern was obtained at room temperature with a step size of 0.005° over the 2θ range 2–100°. The sample was forced to revolve during the pattern acquisition in order to avoid damage by the X-ray beam. A grinding procedure was not applied to **F_1**, in order to avoid possible transformation of the molecular packing structure by external forces. As a result, a preferred orientation was expected because of the plate shape of the sample.

PXRD data analysis of F_1

Structure determination from powder diffraction data process was performed using the high-resolution diffraction pattern of **F_1**. The peak indexing process was performed using the *Crysfire* program.[10] Through this process, a primitive tetragonal unit cell was obtained. This cell was further refined to $a = b$ = 10.43481(4) Å, c = 45.02308(20) Å, $\alpha = \beta = \gamma$ = 90°, V = 4902.35(4) Å^3 during the Rietveld refinement process (Fig. S3). Considering the volume of the molecule itself and the volume of the unit cell, the Z value was expected to be 4, so that space group of the unit cell was predicted as $P4_1$ or $P4_3$; only $P4_3$ space group was determined to be suitable one for **F_1** during the Rietveld refinement procedure.

The molecular geometry employed in the PXRD structure determination process was adopted from the single crystal structure. The model was then converted to a Fenske-Hall Z-matrix using *Openbabel*[11] software. In the calculation using the *F.O.X.*[12, 13] program, this transformed matrix was used as a molecular model. Max sin θ/λ was 0.33, which is equivalent to 1.5 Å maximum resolution. Restraints on bond distances and angles, including intramolecular hydrogen bonds, were established based on a *Mogul*[14, 15] molecular geometry check of the CCDC data base. The anti-bump parameters to prevent intermolecular collisions in the structure solution were set at the Van der Waals radius of the individual atoms making up the molecule. A single temperature displacement factor was refined using Global B_{iso} parameter. The March-Dollase preferred orientation model[16] was applied to the [001] direction to approximate the texture resulting from the plate shape. Parallel tempering was chosen as a method of global optimization, with 10,000,000 cycle calculations per run. Grid computing was used to reduce the time required, and more than 10 independent runs were performed under the same conditions. Among the results, the structure with the lowest cost was used as the initial structure in Rietveld refinement.

Rietveld refinement was carried out using *GSAS*[17] / *EXPGUI*[18] program. In this process, only data range from 6.5° to 60° in 2θ was used, and the d_{min} value was 1.48630 Å. Background intensities in this pattern was manually fitted and subtracted. The pattern was further modeled and refined with sixteen-terms shifted Chebyshev polynomial function. The restraints for bond distances and angles were identical to the structure solution process. Amide groups and aromatic ring geometries were restricted to reproduce atomic hybridization with planar restraints. These restraints were maintained until the end of the refinement, contributing as much as

1.56% of the final reduced χ^2 value. The thermal displacement factors (U_{iso}) were grouped and refined for individual atomic species to ensure secondary structural flexibility. Profile function No.4 for the constant wavelength X-ray data in *GSAS* was used, which contains the Stephens anisotropic microstrain model.[19] In total 220 parameters were refined using 10883 observations and 183 restraints, resulting R_p = 0.0596, R_{wp} = 0.0802, and goodness of fit S = 2.27. The final Rietveld plot is represented in Fig. S4. Crystallographic parameters and atomic coordinates are represented in Table S2 and Table S3, respectively.

Supplementary figures

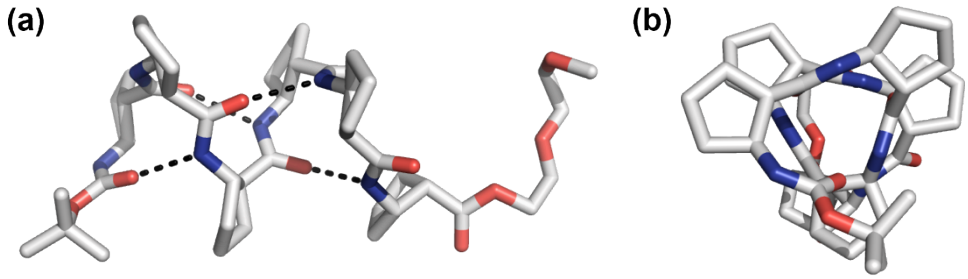

Fig. S1 Single crystal structure of $\mathbf{P_1}$ viewed along the (a) lateral and (b) axial directions. Hydrogen atoms are omitted for clarity. In (a), Intramolecular hydrogen bonds are shown as dashed lines. Carbon, nitrogen and oxygen atoms are colored in dark gray, blue, and red, respectively.

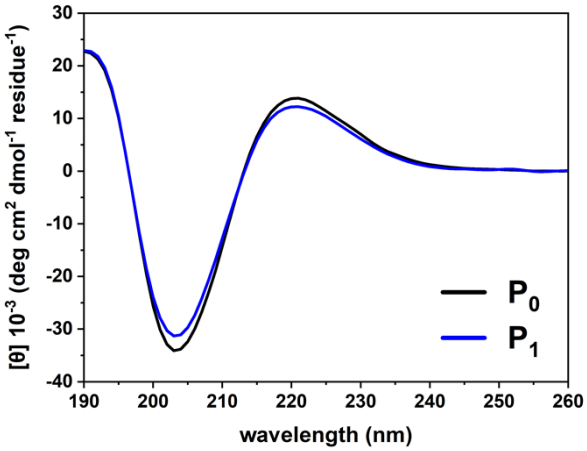

Fig. S2 Circular dichroism spectra of (black line) $\mathbf{P_0}$ and (blue line) $\mathbf{P_1}$ (1 mM in methanol, 0.1 mm path length, 298K).

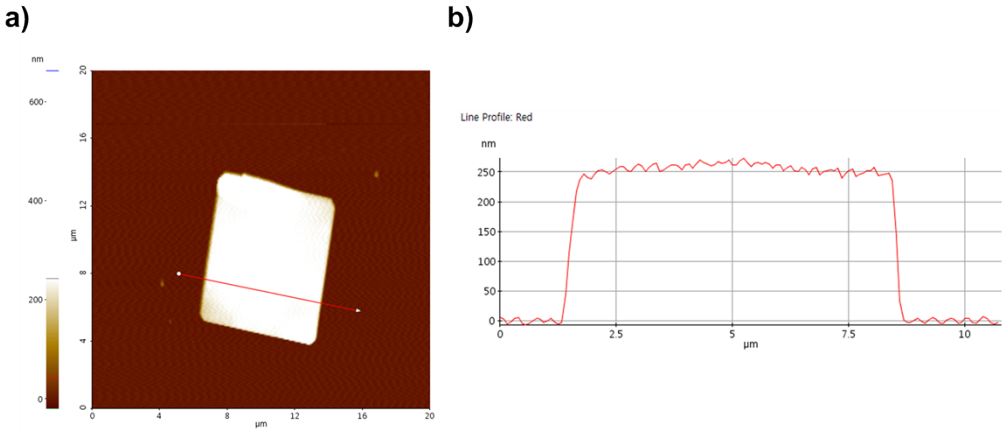

Fig. S3 (a) AFM image and (b) corresponding height profile of $\mathbf{F_1}$.

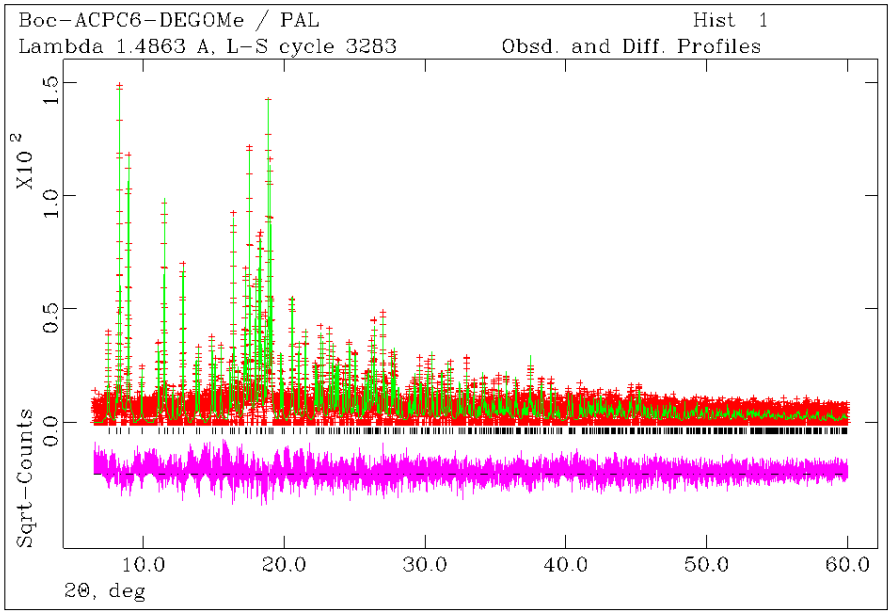

Fig. S4 The final Rietveld plot of $\mathbf{F_1}$. In this plot, red crosses represent the observed intensity, green line represents the calculated intensity, pink curve represents the difference between the observed intensity and the calculated intensity, and the black tick marks represent the expected peak positions predicted by Bragg's law. The scale on the y-axis was transformed to a square-root scale so that high-angle data can be seen clearly.

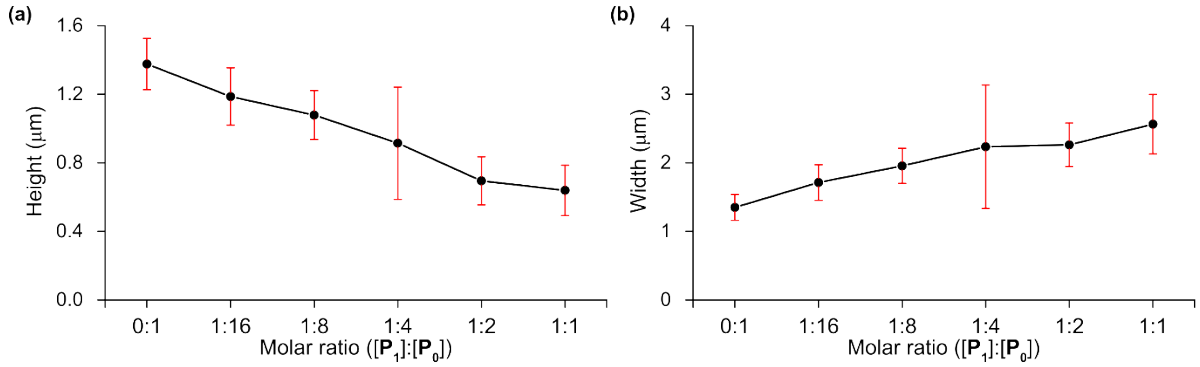

Fig. S5 (a) Height and (b) width profiles of co-assemblies as a function of foldamer molar ratio, with error bars representing standard deviations.

a)

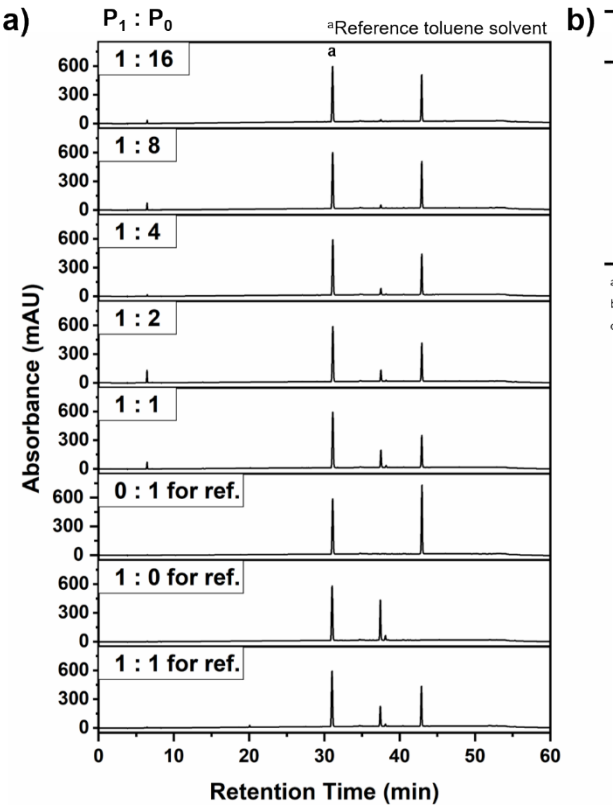

b)

Entry	Condition[a]		Relative area (%)[a]		Molar ratio[a,b]	
1	1	16	3.05	96.65	1	16.30
2	1	8	5.93	94.07	1	8.13
3	1	4	12.47	87.53	1	3.60
4	1	2	21.59	78.41	1	1.86
5	1	1	34.43	65.57	1	0.98
6[c]	1	1	33.61	66.39	–	–

[a]Left is $\mathbf{P_1}$ and right is $\mathbf{P_0}$.
[b]Molar ratio calculated by a reference sample.
[c]Reference sample consists of 1 : 1 ratio of $\mathbf{P_1}$: $\mathbf{P_0}$

Fig. S6 (a) HPLC profiles of (top five rows) co-assembled structures and (bottom three rows) solutions of $\mathbf{P_0}$ and $\mathbf{P_1}$ at different molar ratios. Toluene (peak a) was added as an internal reference. (b) Table showing the relative peak area of $\mathbf{P_0}$ and $\mathbf{P_1}$ in the HPLC profiles in (a). The molar ratio of each peptide in the co-assembled structures was calculated from entry 6.

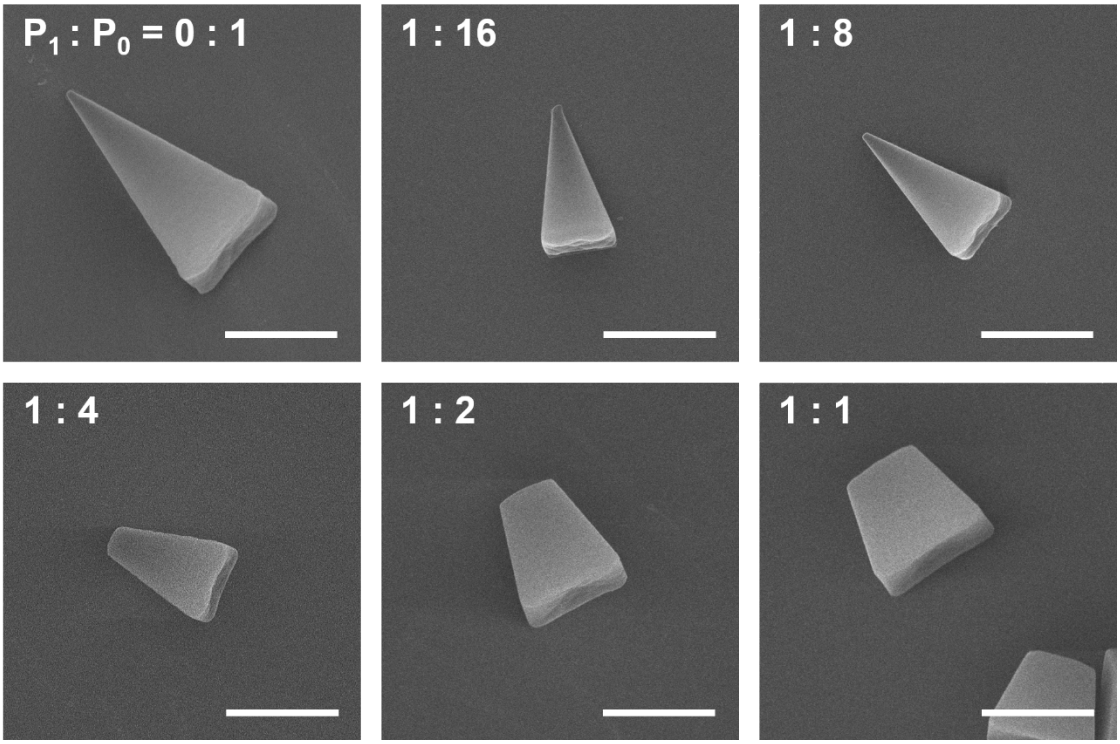

Fig. S7 SEM images of co-assembled structures of $\mathbf{P_0}$ and $\mathbf{P_1}$ at different molar ratios in aqueous CTAB solutions (scale bars = 1 μm).

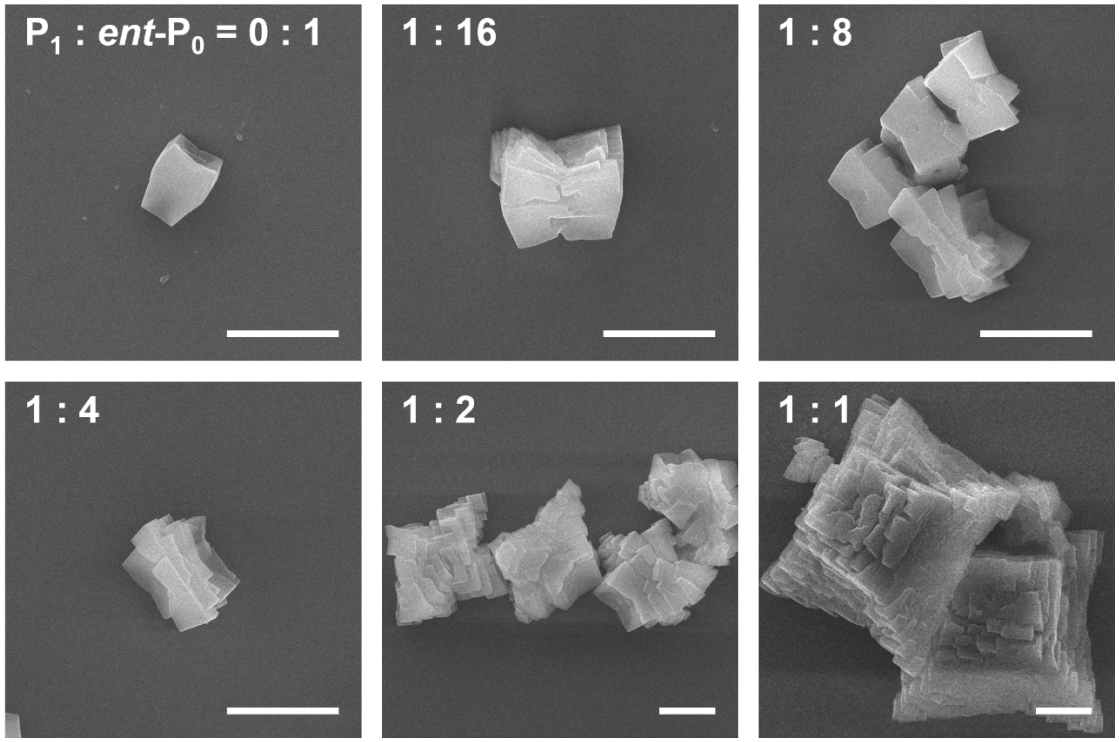

Fig. S8 SEM images of co-assembled structures of ***ent*-$\mathbf{P_0}$** and $\mathbf{P_1}$ at different molar ratios in aqueous P123 (scale bars = 2 μm, ***ent*-$\mathbf{P_0}$** = Boc–(*R,R*)-$ACPC_6$–OBn).

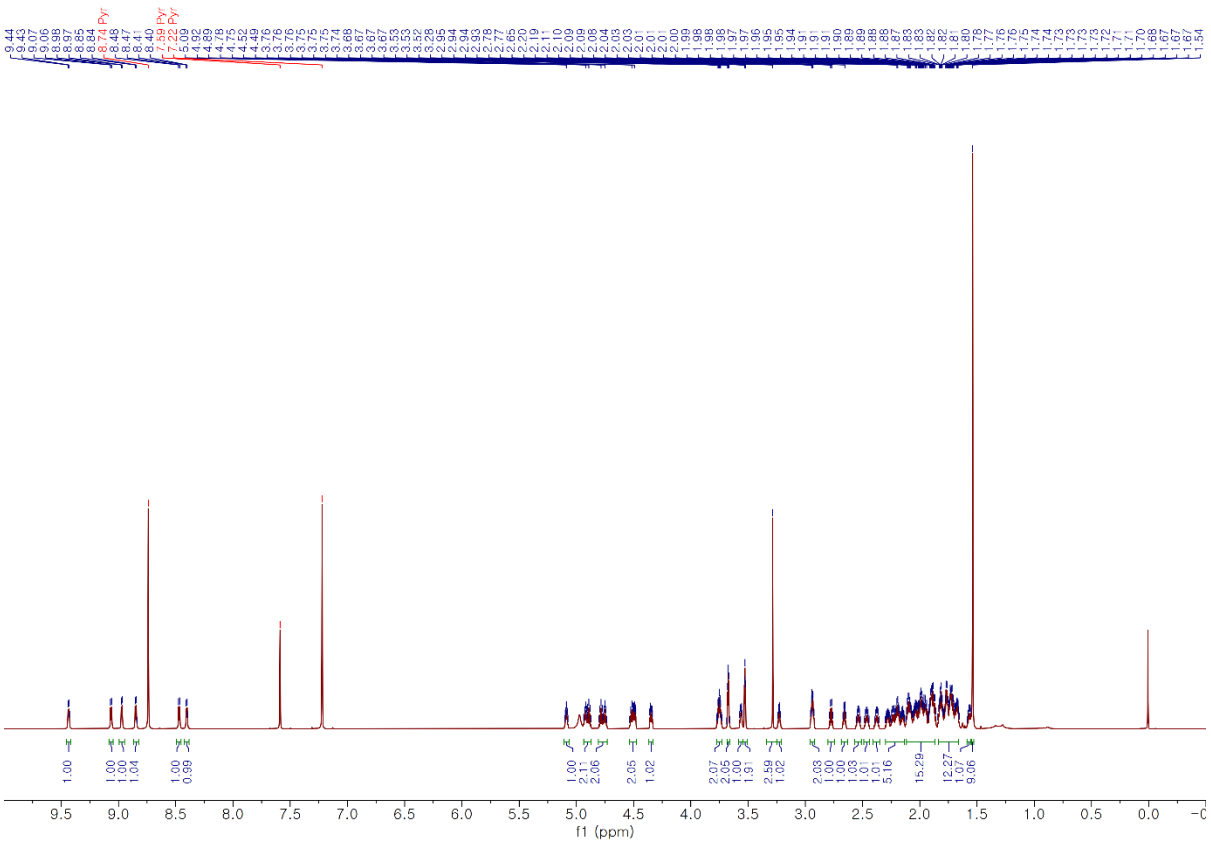

Fig. S9 ^{1}H NMR spectrum of $\mathbf{P_1}$ (900 MHz, in pyridine-d_5, 298 K, 10 mM).

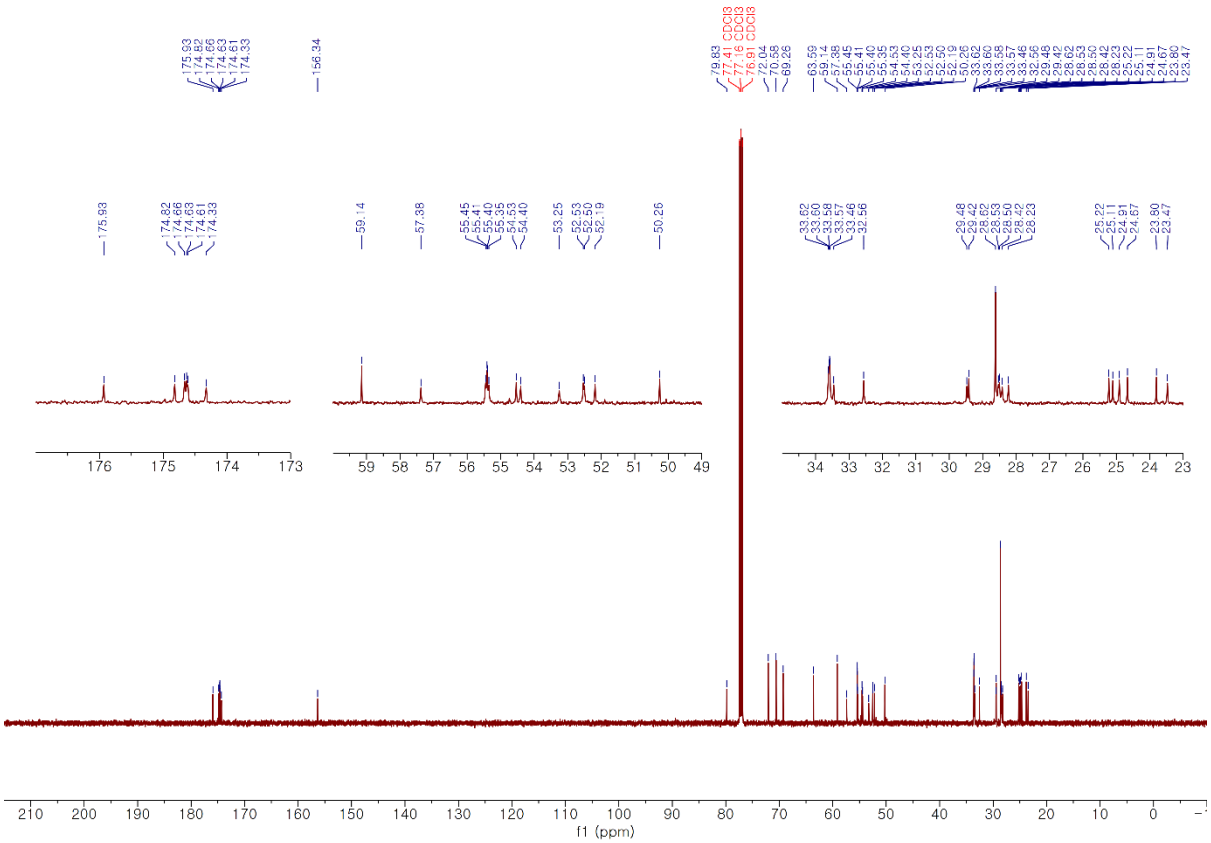

Fig. S10 ^{13}C NMR spectrum of $\mathbf{P_1}$ (126 MHz, in chloroform-*d*, 298 K, 40 mM).

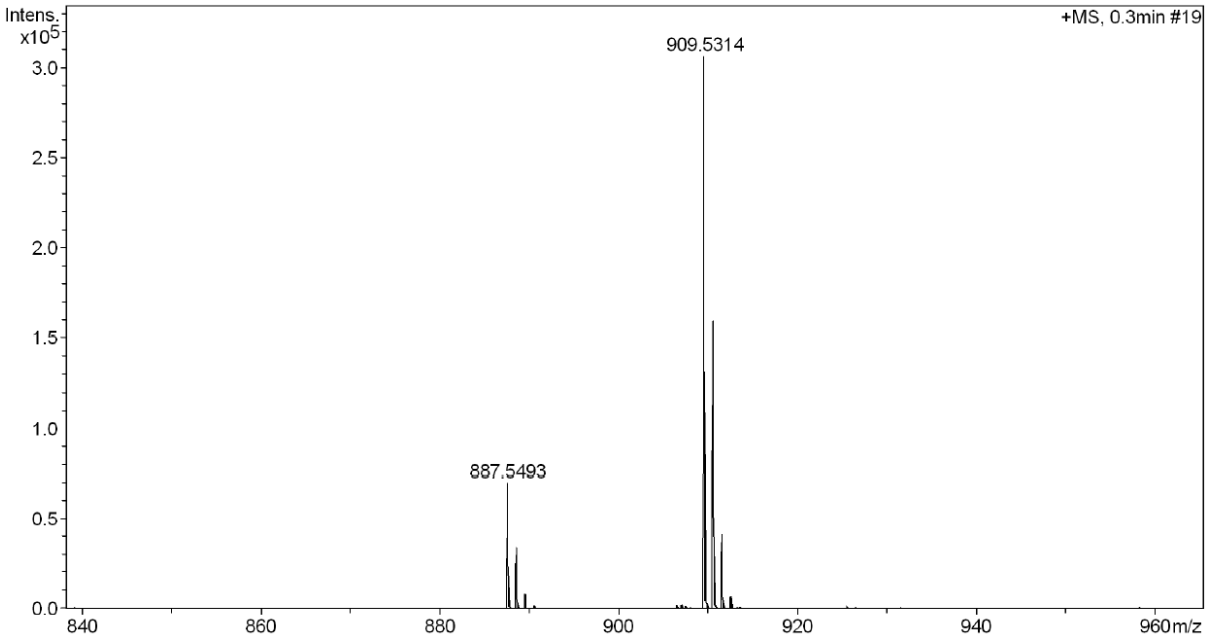

Fig. S11 HRMS profile of **P_1** ((ESI+) calcd. for $C_{46}H_{74}N_6O_{11}Na$ $[M+Na]^+$ 909.5308, found 909.5314).

Supplementary tables

Table S1 Crystallographic information used for single crystal X-ray analysis of $\mathbf{P_1}$.

Crystal Data	$\mathbf{P_1}$
Empirical formula	$C_{46}H_{74}N_6O_{11}$
Formula weight	887.11
Temperature/K	200.00
Crystal system	tetragonal
Space group	$P4_3$
a/Å	10.346(3)
b/Å	10.346
c/Å	44.580(15)
α/°	90
β/°	90
γ/°	90
Volume/Å^3	4772(4)
Z	4
ρ_{calc}g/cm^3	1.235
μ/mm^{-1}	0.088
F(000)	1920.0
Crystal size/mm^3	0.27 × 0.15 × 0.03
Data Collection	
Radiation	MoKα (λ = 0.71073)
2Θ range for data collection/°	3.936 to 56.77
Index ranges	-13 ≤ h ≤ 13, -13 ≤ k ≤ 13, -59 ≤ l ≤ 59
Reflections collected	91991
Independent reflections	11874 [R_{int} = 0.0700, R_{sigma} = 0.0433]
Refinement	
Data/restraints/parameters	11874/1488/680
Goodness-of-fit on F^2	1.302
Final R indexes [I>=2σ (I)]	R_1 = 0.1126, wR_2 = 0.3118
Final R indexes [all data]	R_1 = 0.1375, wR_2 = 0.3379
Largest diff. peak/hole / e Å^{-3}	0.75/-0.45
Flack parameter	-0.1(3)

Table S2 Crystallographic information used for powder X-ray analysis of $\mathbf{F_1}$.

Crystal data	
Chemical formula*	$C_{46}N_6O_{11}$
M_r (g/mole)*	812.54
Crystal system, space group	Tetragonal, $P4_3$
$a = b$, c (Å)	10.43442 (4), 45.02143 (20)
α, β, γ (°)	90, 90, 90
V (Å^3)	4901.80 (4)
Z, Z'	4, 1
Radiation type	synchrotron radiation (λ = 1.4863 Å)
Temperature (K)	298
Data collection	
Instrument	Pohang Accelerator Laboratory 9B High-resolution Powder Diffraction Beamline (PAL Pohang, Republic of Korea)
2ϑ (°, range in Refinement)	$2\vartheta_{min}$ = 6.5, $2\vartheta_{max}$ = 60, increment = 0.005
Refinement	
Least-squares matrix	Full-matrix
R factors and *goodness of fit*	R_p = 0.0596, R_{wp} = 0.0802, R_{exp} = 0.0356 and S = 2.27
Profile function	CW Profile function number 4 with 17 terms. Pseudo-voigt profile coefficients as parameterized in Tompson *et al*. (1987). Asymmetry correction of Finger *et al*. (1994). Microstrain broadening by Stephens *et al.* (1999). #1(GU) = 0.000, #2(GV) = 0.000, #3(GW) = 0.000, #4(GP) = 0.000, #5(LX) = 0.668, #6(ptec) = 0.83, #7(trns) = 25.00, #8(shft) = −0.7763, #9(sfec) = 0.00, #10(S/L) = 0.0097, #11(H/L) = 0.0096, #12(eta) = 0.4721, #13(S400) = 3.6×10^{-3}, #14(S004) = 0.000, #15(S220) = 3.2×10^{-3}, #16(S202) = 0.000, #17(S310) = 0.000. Peak tails are ignored where the intensity is below 0.0010 times the peak. Anisotropic broadening axis 0.0 0.0 1.0
Treatment of preferred orientation	March-Dollase model, axis setting = [hkl] = [004], P_{MD} = 0.98692
No. of parameters	221
No. of restraints	183
No. of data points	10701
Background function	16-terms of Shifted Chebyshev function. 1: 642.591, 2:2.97602, 3:-11.4253, 4:-0.937278, 5:-1.76901, 6:5.75617, 7:1.01367, 8:-1.81634, 9:0.496022, 10:0.594641, 11:-1.89514, 12:-1.24261, 13:-1.85364, 14:1.93726, 15:-0.746287, 16:-0.579458
$(\Delta/\sigma)_{max}$	0.06

*All-hydrogen atoms were omitted during the structure determination process due to the weak contribution of H atoms to X-ray diffraction.

Table S3 Atomic coordinates, displacement parameters and population parameters of $\mathbf{F_1}$.

Entry	Label	Occupancy	Multiplicity	*x*	*y*	*z*	U_{eq} (Å)
1	O1	1	4	0.7286(18)	0.4313(13)	0.4334(13)	0.141
2	C2	1	4	0.7107(13)	0.4170(8)	0.40690(13)	0.0958
3	N3	1	4	0.7551(14)	0.3126(10)	0.39220(18)	0.104
4	C4	1	4	0.8165(9)	0.2047(8)	0.40743(19)	0.0958
5	C5	1	4	0.9650(9)	0.2169(8)	0.40871(18)	0.0958
6	C6	1	4	1.0079(14)	0.2870(8)	0.43661(14)	0.0958
7	O7	1	4	0.9981(14)	0.2364(12)	0.46122(9)	0.141
8	N8	1	4	1.0636(14)	0.4049(11)	0.43242(17)	0.104
9	C9	1	4	1.1081(9)	0.4905(9)	0.45648(19)	0.0958
10	C10	1	4	1.0082(8)	0.5963(9)	0.46523(18)	0.0958
11	C11	1	4	0.9328(8)	0.5573(15)	0.49260(14)	0.0958
12	N12	1	4	0.8091(10)	0.5259(15)	0.48862(17)	0.104
13	C13	1	4	0.7245(8)	0.4830(9)	0.51250(19)	0.0958
14	C14	1	4	0.7243(8)	0.3356(9)	0.51686(18)	0.0958
15	C15	1	4	0.8250(8)	0.2936(13)	0.53860(14)	0.0958
16	N16	1	4	0.9289(9)	0.2333(14)	0.52696(9)	0.104
17	C17	1	4	1.0323(8)	0.1835(8)	0.54525(19)	0.0958
18	C18	1	4	1.2137(10)	0.3269(7)	0.55916(17)	0.0958
19	C19	1	4	1.2501(12)	0.1177(13)	0.53297(27)	0.0958
20	C20	1	4	1.1589(18)	0.0128(16)	0.52558(27)	0.0958
21	C21	1	4	1.0440(15)	0.0374(10)	0.54378(26)	0.0958
22	O22	1	4	0.8061(13)	0.3013(19)	0.56532(20)	0.141
23	C23	1	4	0.5887(12)	0.3033(14)	0.52779(26)	0.0958
24	C24	1	4	0.5836(11)	0.5147(15)	0.50615(25)	0.0958
25	O25	1	4	0.9814(12)	0.5601(18)	0.51692(19)	0.141
26	C26	1	4	1.0864(15)	0.7211(11)	0.47029(27)	0.0958
27	C27	1	4	1.0171(14)	0.0786(12)	0.40745(26)	0.0958
28	C28	1	4	0.9177(18)	0.0035(16)	0.39106(28)	0.0958
29	C29	1	4	0.7894(13)	0.0754(12)	0.39241(25)	0.0958
30	C30	1	4	0.6487(9)	0.5217(8)	0.38830(18)	0.0958
31	C31	1	4	0.7256(8)	0.6488(8)	0.39061(19)	0.0958
32	N32	1	4	0.8100(11)	0.6693(14)	0.36533(19)	0.104
33	C33	1	4	0.9342(9)	0.6296(13)	0.36537(18)	0.0958
34	O34	1	4	0.9985(10)	0.6757(13)	0.34170(20)	0.141
35	C35	1	4	1.1306(10)	0.6314(12)	0.33475(20)	0.0958
36	C36	1	4	1.2190(21)	0.6904(23)	0.35713(26)	0.0958
37	C37	1	4	1.1699(24)	0.6668(23)	0.30398(24)	0.0958
38	O38	1	4	0.9812(13)	0.5659(16)	0.38469(22)	0.141
39	C39	1	4	0.6259(13)	0.7554(11)	0.39409(28)	0.0958
40	C40	1	4	0.4972(16)	0.6929(17)	0.38960(29)	0.0958
41	C41	1	4	0.5136(12)	0.5560(15)	0.39907(26)	0.0958
42	O42	1	4	0.8911(23)	0.3068(21)	0.72752(28)	0.364
43	C43	1	4	0.9400(24)	0.4912(25)	0.71199(30)	0.364
44	C44	1	4	0.9750(27)	0.4038(27)	0.73506(29)	0.364
45	O45	1	4	1.0304(18)	0.5877(20)	0.71018(30)	0.364
46	C46	1	4	1.1594(21)	0.5504(28)	0.71108(29)	0.364

Entry	Label	Occupancy	Multiplicity	*x*	*y*	*z*	U_{eq} (Å)
47	C47	1	4	1.2309(11)	0.5653(15)	0.44873(24)	0.0958
48	C48	1	4	1.2257(16)	0.6771(18)	0.47042(28)	0.0958
49	C49	1	4	1.1246(25)	0.4888(17)	0.33645(27)	0.0958
50	C50	1	4	1.2147(22)	0.6205(25)	0.68581(26)	0.364
51	C51	1	4	0.9584(34)	0.1976(27)	0.71671(30)	0.364
52	C52	1	4	0.5163(17)	0.4309(18)	0.52776(27)	0.0958
53	C53	1	4	1.1959(10)	0.6093(13)	0.63280(16)	0.0958
54	O54	1	4	1.1501(14)	0.5729(17)	0.65922(20)	0.313
55	C55	1	4	1.1647(8)	0.2360(8)	0.53591(19)	0.0958
56	C56	1	4	1.1220(9)	0.5487(11)	0.60757(17)	0.0958
57	C57	1	4	1.0063(12)	0.6318(16)	0.59920(25)	0.0958
58	C58	1	4	1.0623(18)	0.7343(17)	0.57794(27)	0.0958
59	O59	1	4	1.2759(16)	0.2870(12)	0.58025(21)	0.141
60	N60	1	4	1.1664(12)	0.4478(10)	0.55842(18)	0.104
61	C61	1	4	1.2044(10)	0.5472(8)	0.57920(16)	0.0958
62	C62	1	4	1.1933(17)	0.6837(11)	0.56688(23)	0.0958
63	O63	1	4	1.2954(16)	0.6686(22)	0.62889(25)	0.313

Supplementary references

1. D. H. Appella, L. A. Christianson, D. A. Klein, M. R. Richards, D. R. Powell, and S. H. Gellman, *J. Am. Chem. Soc.*, 1999, **121**, 7574–7581.
2. J. Gong, T. Eom, W. Lee, A. Roy, S. Kwon, H. Kim, and H. S. Lee, *ChemPlusChem*, 2019, **84**, 481–487.
3. J. Hong, W. Lee, and H. S. Lee, *Bull. Korean Chem. Soc.*, 2023, **44**, 1034–1039.
4. S. Kwon, K. Kang, A. Jeon, J. H. Park, I. S. Choi, and H.-S. Lee, *Tetrahedron*, 2012, **68**, 4368–4373.
5. SMART, Version 5.0; Data Collection Software; Bruker AXS, Inc., Madison, WI, 1998.
6. G. M. Sheldrick, SADABS: Program for Absorption Correction with the Bruker SMART System; Universität Göttingen, Göttingen, Germany, 1996.
7. T. R. Schneider, and G. M. Sheldrick, *Acta Cryst.,* 2002, **D58**. 1772–1779.
8. G. M. Sheldrick, *Acta Cryst.,* 2015, **C71**, 3–8.
9. O. V. Dolomanov, L. J. Bourhis, R. J. Gildea, J. A. K. Howard, and H. Puschmann, *J. Appl. Crystallogr*., 2009, **42**, 339–341.
10. R. Shirley, The CRYSFIRE System for Automatic Powder Indexing: User's Manual, The Lattice Press, 41 Guildford Park Avenue, Guildford, Surrey GU2 7NL, England, 2000.
11. N. M. O'Boyle, M. Banck, C. A. James, C. Morley, T. Vandermeersch, and G. R. Hutchison, *Journal of Cheminformatics*, 2011, **3**, 33.
12. V. Favre-Nicolin; and R. Černý, *Z. Kristallogr.*, 2004, **219**, 847–856.
13. R. Černý, and V. Favre-Nicolin, *Powder Diffr.*, 2005, **20**, 359–365.
14. I. J. Bruno, J. C. Cole, M. Kessler, J. Luo, W. D. S. Motherwell, L. H. Purkis, B. R. Smith, R. Taylor, R. I. Cooper, S. E. Harris, and A. G. Orpen, *J. Chem. Inf. Comput. Sci*, 2004, **44**, 2133–2144.
15. R. A. Sykes, P. McCabe, F. H. Allen, G. M. Battle, I. J. Bruno, and P. A. Wood, *J. Appl. Crystallogr.*, 2011, **44**, 882-886.
16. W. A. Dollase, *J. Appl. Crystallogr.*, 1986, **19**, 267–272.
17. A. C. Larson, and R. B. Von Dreele, General Structure Analysis System (GSAS), Los Alamos National Laboratory Report LAUR 86–784, 2004.
18. B. Toby, *J. Appl. Crystallogr.*, 2001, **34**, 210–213.
19. P. W. Stephens, *J. Appl. Crystallogr.*, 1999, **32**, 281–289.